



J. Serb. Chem. Soc. 85 (6) 751–764 (2020)
JSCS–5336

Binuclear copper(II) complexes: Synthesis, structural characterization, DNA binding and *in silico* studies

ABDUL WAHEED KAMRAN¹, SAQIB ALI^{2*}, MUHAMMAD NAWAZ TAHIR³,
MUHAMMAD ZAHOOR^{1**}, ABDUL WADOOD⁴ AND MUHAMMAD IQBAL^{5***}

¹Department of Chemistry, University of Malakand, Chakdara, Dir(L) KPK, Pakistan,

²Department of Chemistry Quaid-i-Azam University, Islamabad 45320, Pakistan,

³Department of Physics, University of Sargodha, Sargodha, Pakistan, ⁴Department of Biochemistry, Abdul Wali Khan University, Mardan, KPK, Pakistan and ⁵Department of Chemistry Bacha Khan University Charsadda 24420, KPK, Pakistan

(Received 15 July, revised 30 September, accepted 10 October 2019)

Abstract: Two new binuclear Cu(II) complexes represented by the general formula $\{(dmsO)Cu(\mu-L)_4Cu(dmsO)\}$ (**1**) and $\{(Phen)(L)Cu(\mu-L)_2Cu(L)(Phen)\}$ (**2**) where dmsO = dimethyl sulphoxide, L = 2-bromophenyl acetate and Phen = 1,10-phenanthroline have been synthesized, isolated quantitatively and characterized by UV/Vis and FT-IR spectroscopic techniques, thermogravimetry/differential thermal analysis and X-ray single crystal XRD studies. Complex **1** is paddlewheel with 1,2-*O,O*-bridging while **2** has 1,1-*O*-bridging. The values of the intrinsic binding constants with DNA were found out to be 2.0×10^3 and 1.1×10^3 M⁻¹, respectively for compound **1** and **2**. The mode of interaction of complexes with DNA was also evaluated through computational study by molecular docking (*in silico*) study using molecular operating environment (MOE) software. The synthesized complexes are structurally as well as biologically important.

Keywords: crystal structures; DNA interaction; molecular docking.

INTRODUCTION

The wide range application of copper compounds and their role as micro-nutrients beneficial to organisms have attracted the inorganic chemists for the synthesis of their complexes.¹ The copper complexes play an important role as catalyst in the synthesis of optically active compounds.² The polynuclear copper complexes have found applications in synthesis of organic compounds⁴ and exhibit anti-inflammatory activity.⁵ as well as photoluminescence behavior.³ The deficiency and excess of copper in the body is responsible for disorders, for

*,**,*** Corresponding authors. E-mail: (*)saqibali@qau.edu.pk;

(**)mohammadzahoorus@yahoo.com; (***)iqbalmo@yahoo.com, iqbal@bkuc.edu.pk

<https://doi.org/10.2298/JSC190715109K>

example Wilson's and Menkes.⁶ Copper complexes also play an important role in the proper functioning of several enzymes and proteins responsible for energy metabolism, respiration and DNA synthesis.⁷

Copper complexes incorporating carboxylate ligands are used in the production of thin film in semiconductor industry involving chemical vapor deposition method.⁸ The copper complexes bearing carboxylate functionality and phenanthroline ligands show DNA binding affinity.⁹ The small changes in the structure of ligands around copper greatly alter the electronic and magnetic behaviors of the resulting complexes.¹⁰ The phenanthroline bearing copper complexes show chemical nuclease activity and are used in DNA oxidative cleavage in the presence of a reducing agent.¹¹ Phenanthroline and its derivatives are used as chelating agents for metal determination in analytical chemistry.¹² The molecular docking is used to model the interaction of the synthesized complexes with DNA, which gives information about the conformational changes in ligand and DNA when interact with each other.¹³

Bromophenyl acetate is the derivative of the general class of phenyl acetic acid, which plays an important role in the growth of plants like auxin.¹⁴ It is also used in the synthesis of non-steroidal anti-inflammatory drugs like diclofenac (voltaren), which have analgesic, antipyretic and anti-inflammatory effect through cyclooxygenase inhibition.¹⁵ The dinuclear copper(II) complexes containing planar aromatic heterocyclic ligands show pronounced DNA cleavage activities as compared to the corresponding mononuclear copper(II) complexes.¹⁶ The mononuclear copper(II) complexes with phenanthroline ligand also show DNA binding activities but their DNA binding affinities are lesser than dinuclear copper(II) complexes.¹⁷ The phenanthroline ligand, due to presence of aromatic ring in their chemical structure and hydrophobic nature, enhances the DNA binding affinities of the complexes.¹⁸ The high level of copper in human body can promote cancer, metastasis, and angiogenesis. As a strategy, scientists have synthesized the copper chelator to remove the excess copper from body.¹⁹

Keeping in view the above mentioned applications and uses of copper complexes in various fields, we have synthesized binuclear copper complexes with carboxylate ligands and 1,10-phenanthroline. The complexes were structurally characterized through various spectroscopic techniques and their DNA binding affinities were determined experimentally through absorption spectroscopy and theoretically through computational approach of molecular docking.

EXPERIMENTAL

Materials and methods

Analytical grade anhydrous CuSO_4 , 2-bromophenyl acetate, 1,10-phenanthroline, sodium bicarbonate and potassium chloride were obtained from Fluka, USA, and were used as received. Methanol and dimethyl sulphoxide (DMSO) were of analytical grade. The water used in the experiment was singly distilled. The melting points were determined in a capillary

tube using a Gallenkamp, serial number C040281, UK, electro-thermal melting point apparatus. FT-IR spectra were obtained on a Nicolet-6700 FT-IR spectrophotometer, thermoscientific, USA, in the range from 4000 to 400 cm^{-1} .

X-ray crystallographic studies

The crystallographic data were obtained at 293 K using an Oxford diffraction Gemini ultra CCD diffractometer using graphite monochromated Mo-K α radiation ($\lambda = 0.071073$ nm). Data reduction and empirical absorption correction completed through CrysAlisPro (Oxford diffraction, version 171.33.66). The structures of the complexes were solved by direct method with SHLEX-86 and refined by full matrix least square analysis against F^2 with SHLEX-97²⁰ within WinGX package.²¹ ORTEP3 was used for drawing the structures of complexes.²²

The data of both crystals has been deposited with CCDC 1880878 and 1880879 corresponding to **1** and **2**, respectively.

DNA interaction study by absorption spectroscopy

Solutions of complexes were prepared with 8 mM concentration in aqueous DMSO (1:4) for UV/Vis analysis. The absorption spectra were determined by titrating the complexes against different concentrations of salmon sperm DNA (SSDNA). The solutions were allowed at ambient temperature to ensure the complete mixing of complexes with SSDNA. The cuvettes of 1.0 cm path length were used for recording the absorption spectra.

Synthetic procedure for the complexes

Complex **1** was prepared by treating 2-bromophenyl acetic acid (8.0 mmol, 1.72 g) with NaHCO_3 (8.0 mmol, 0.672 g) in distilled water at 50 °C. After completion of neutralization, aqueous solution of CuSO_4 (4.0 mmol, 0.636 g) was added and the reaction mixture was stirred for 2 h at 50 °C as shown in Scheme S-1 of the Supplementary material to this paper. The final product was filtered, washed with distilled water, dried and recrystallized from dimethyl sulfoxide and characterized by FT-IR and single crystal analysis.

Complex 1. Dark blue color; m.p. 249–250 °C; yield (71 %). $\lambda_{\text{max}} = 651$ nm. $\epsilon = 48$ L $\text{mol}^{-1} \text{cm}^{-1}$. FT-IR: 1632 cm^{-1} $\nu(\text{C}=\text{O})_{\text{asym}}$, 1389 cm^{-1} $\nu(\text{C}=\text{O})_{\text{sym}}$, $\Delta\nu$: 243 cm^{-1} , 416 cm^{-1} $\nu(\text{Cu}-\text{O})$.

Complex **2** was prepared by treating 2-bromophenyl acetic acid (8.0 mmol, 1.72 g) with NaHCO_3 (8.0 mmol, 0.672 g) in distilled water at 50 °C. After completion of neutralization, aqueous solution of CuSO_4 (4.0 mmol, 0.636 g) was added and the reaction mixture was stirred for 2 h at 50 °C; then solid 1,10-phenanthroline (4.0 mmol, 0.72 g) was added and stirred for another 2 h as shown in Scheme S-2 of the Supplementary material. The final product was filtered, washed with distilled water and air dried. The solid was recrystallized from methanol and characterized by FT-IR and X-ray analysis.

Complex 2. Light blue color; m.p. 203–204 °C; yield (65 %). $\lambda_{\text{max}} = 671$ nm. $\epsilon = 39$ L $\text{mol}^{-1} \text{cm}^{-1}$. FT-IR: 1606 cm^{-1} $\nu(\text{C}=\text{O})_{\text{asym}}$, 1364 cm^{-1} $\nu(\text{C}=\text{O})_{\text{sym}}$, $\Delta\nu$: 242 cm^{-1} , 470 cm^{-1} $\nu(\text{Cu}-\text{N})$, 429 cm^{-1} $\nu(\text{Cu}-\text{O})$.

Both complexes are soluble in common solvents like methanol, ethanol, chloroform, acetone, DMSO, partially soluble in ether and insoluble in pure water.

Molecular docking

The three dimensional (3D) structures of the newly synthesized Cu-complexes were drawn by molecular operating environment (MOE-2016) software.²³ The hydrogen atoms were added to the synthesized compounds by 3D protonation followed by energy mini-

mization using MOE. The crystal structure of the double stranded DNA dodecamer was retrieved from the protein databank (PDB id: 1BNA, www.rcsb.org/pdb). Prior to molecular docking, all water molecules were removed from the retrieved crystal structure using the MOE software. The 3D protonation and energy minimization of the retrieved DNA was carried out by using MOE software. The macromolecule (DNA) was allowed to dock to the synthesized copper complexes using MOE. For each ligand ten conformations were generated. The top-ranked conformation of each complex was used for further analysis.

RESULTS AND DISCUSSION

FTIR data

Both the complexes were characterized by FTIR spectrophotometer, which showed all characteristic absorption bands in the spectrum.

The complex **1** showed peak at 1632 cm^{-1} corresponding to the asymmetric (C=O) stretching frequency and a symmetric stretching peak of (C=O) at 1389 cm^{-1} . The Cu–O peak of carboxylate appeared at 416 cm^{-1} .²⁴ The IR spectroscopy is a powerful tool for determining the coordinating mode of COO moiety in metal carboxylate complexes, the difference between asymmetric and symmetric stretching frequencies, *i.e.*, $\Delta\nu(\nu_{\text{asym}}(\text{OCO})-\nu_{\text{sym}}(\text{OCO}))$ less than 150 cm^{-1} corresponds to a chelate nature, greater than 250 cm^{-1} shows a monodentate carboxylate moiety and value between 150 and 250 cm^{-1} indicates a bridging behavior.²⁵ The $\Delta\nu$ value for complex **1** was 243 cm^{-1} that shows a bridging coordination mode of the carboxylate group which was further confirmed by the structural studies.

The complex **2** showed peak at 1606 cm^{-1} corresponding to the asymmetric stretching of C=O and 1364 cm^{-1} which is symmetric stretching frequency of C=O functionality of the carboxylate ligand. The Cu–N bond vibration was found at 470 cm^{-1} . The appearance of a Cu–O absorption band at 429 cm^{-1} is an indication for the coordination of carboxylate through oxygen. The $\Delta\nu$ value of 242 cm^{-1} corresponds to the bridging behavior of carboxylate group in line with the XRD data.

Crystal structure description

The ORTEP diagram for the complex **1** is shown in Fig. 1. The crystal refinement parameters and important bond lengths and angles are given in Tables S-I and S-II of the Supplementary material. The molecule belongs to space group *P*-1. The complex is in the dimeric form, in which each Cu is in five coordinated square pyramidal environment. The four oxygen atoms of the carboxylates around each Cu(II) occupy the square planar position while the DMSO oxygen occupies the apical position of the square pyramid. The Cu...Cu and average Cu–O (equatorial) bond distances are 2.649 and 1.965 Å, respectively, which are closely related to the bond distances of Cu(II) complexes reported in the literature.²⁶ The Cu–O bond distances are asymmetrical in the equatorial plane and are

shorter compared to the axial Cu–O bond (2.153(2) Å) as are reported for the structurally similar dimeric Cu(II) complexes.²⁷ The axial Cu–O bond distance is 2.1529(2) Å and shows a weak interaction with copper. The elongation of apical bond is due to the occupancy of anti-bonding a_1 orbital (d_z^2) by two electrons resulting in a high electron cloud along the Cu–O axial bond.²⁸ The $d_{x^2-y^2}$ orbital is singly occupied and therefore the ligands experience lesser repulsion from the metal electron and come closer to it in the equatorial plane. The O_1 –Cu₁– O_3 angle for the complex is 90.1(1)°, the O_1 –Cu₁– O_5 angle is 98.9(1)°, the O_1 –Cu₁– O_2 is 167.8(1)°, O_3 –Cu₁– O_4 angle is also 167.9(1)°. These data clearly show the square pyramidal geometry for the complex **1**.

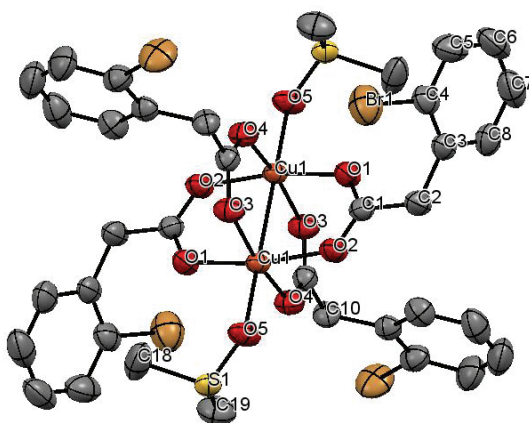


Fig. 1. ORTEP diagram for complex **1**.

Fig. 2 represents the packing diagram for complex **1** and shows that the intermolecular interactions comprise mostly of $C \cdots H-C$, $O \cdots H-C$ and $S \cdots H-C$ type interactions. These weaker linkages arise because the molecule has no polar hydrogen to result in true hydrogen bonding.

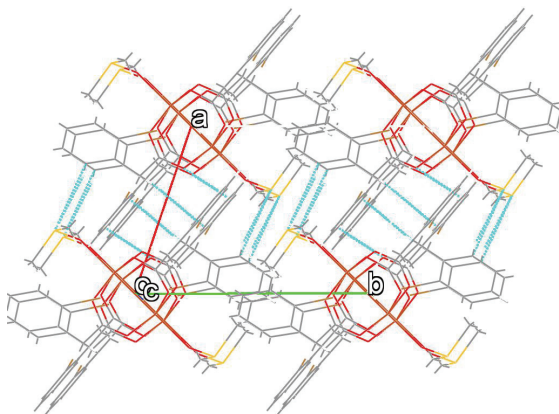


Fig. 2. Packing diagram of complex **1** as viewed along c -axis.

The ORTEP diagram for complex **2** is shown in Fig. 3. The complex belongs to space group $C2/c$ and is composed of dimeric units, where each copper atom is surrounded by five donor atoms adopting square pyramidal geometry. The two nitrogen atoms of phenanthroline and two oxygen atoms of two carboxylates occupy the equatorial position, while the third carboxylate containing bridging oxygen atom occupies the axial position.

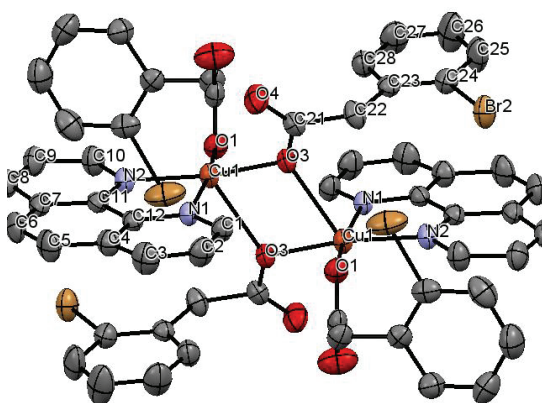


Fig. 3. ORTEP diagram for complex **2**.

The two Cu–N bonds in the plane are 2.037(2) Å each and the two Cu–O bonds from the two carboxylates moiety in the plane are 1.930(1) and 1.955(2) Å, while the apical Cu–O bond distance is 2.455(2) Å and mostly similar to the dinuclear Cu(II) complexes reported in the literature.²⁹ The geometry around copper is less distorted square pyramidal than that of the complex **1** owing partly to the asymmetric bridging nature of the 1,1-*O*-bridging oxygen atom. The elongation of axial bond along axial position is due to accommodation of two electrons in the a_1 (d_{z^2}) orbital, which does not allow the close approach of the ligands along z -axis while the $d_{x^2-y^2}$ orbital having b_1 symmetry is singly occupied and presents minimum repulsion to the approaching ligands along x - and y -axes. This results in closer ligand approach and consequently shorter bond length. The O₁–Cu₁–O₃ bond angle is 95.96(9)°, the O₁–Cu₁–N₁ angle is 169.1(1)°, the O₁–Cu₁–N₂ angle is 89.7(1)°, O₁–Cu₁–O₃ angle is 88.10(8)°, O₃–Cu₁–N₁ angle is 94.50(9)° and the O₃–Cu₁–N₂ angle is 168.4(1)°. These data indicate square pyramidal geometry for complex **2**.

The axial bond elongation with respect to equatorial bond length is in close agreement with the complexes already reported. The greater separation in bond length between two Cu(II) ion with respect to Cu–O and Cu–N bond length is due to the nonexistence of actual bond between two Cu(II) ions. Each Cu(II) ion has unpaired electron in the $d_{x^2-y^2}$ orbital, which is not properly oriented for Cu–Cu bond formation. While the d_{z^2} orbital on each copper ion are pointing the right way for Cu–Cu bond formation, however these orbitals are fully populated

with electron pair. Therefore the Cu–Cu bond can't exist in such dinuclear Cu(II) complexes.³⁰

The supramolecular structure of the complex **2** has been given in Fig. 4 showing that the molecules are held together through weak Br···H–C and O···H–C type linkages. Again here, there is no polar hydrogen and thus no H-bonding in the lattice of **2**.

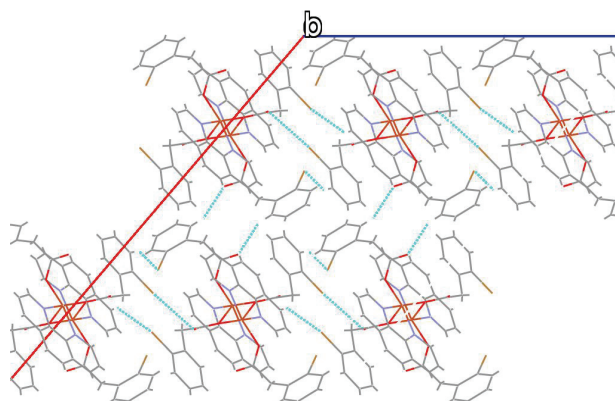


Fig. 4. Packing diagram of complex **2** as viewed along *b*-axis.

The copper atoms in both complexes are indicated as Cu1, because the geometry around each copper is the same hence both are chemically identical and the complex is centrosymmetric.

Thermogravimetric analysis

Fig. S-1 of the Supplementary material shows the thermogravimetric curve of complex **1** that contains three decomposition steps. The complex is stable below 80 °C and above this temperature water molecule is lost (weight loss: calculated, 16.55 %; observed 16.18 %). The decomposition of monodentate carboxylate ligand occurs in the range of 220–260 °C (weight loss: calculated, 42.48 %; observed, 42.43 %), while the most strongly bonded copper oxide decomposed between 500–710 °C corresponding to a total weight loss of 24.0 % (calculated 23.44 %). The accumulative observed weight loss was 82.25 %. The weight of the final residue is 17.30 % of the total weight. Thermogravimetric plot of complex **2** has been given in Fig. S-2 of the Supplementary material which shows two decomposition steps. The complex is stable up to 80 °C and the loss of water molecule started above 80 °C and completed at 120 °C (weight loss: calculated, 17 %; observed, 16.70 %). Monodentate carboxylate ligands decomposed in temperature range 220–260 °C (weight loss: calculated, 42.40 %; observed 42.41 %). However, more refractory copper oxide has been found to decompose between 500–710 °C range corresponding to a total weight loss of

24.0 % (calculated 23.41 %). The accumulative observed weight loss was 82.60 %. The final residue weight is 17.30 % of the total weight.

Absorption spectroscopy

The absorption spectrum of the complex **1** is shown in Fig. 5A and exhibits peak in the visible region having $\lambda_{\max} = 277$ nm corresponding to π - π transition due to the presence of aromatic ligand in the complex. The complex also shows a small peak in the in 498 nm visible region due to d-d transition. This absorption band is typical of distorted octahedral geometry in solution form, where the DMSO solvent molecule acts as ligand.³¹

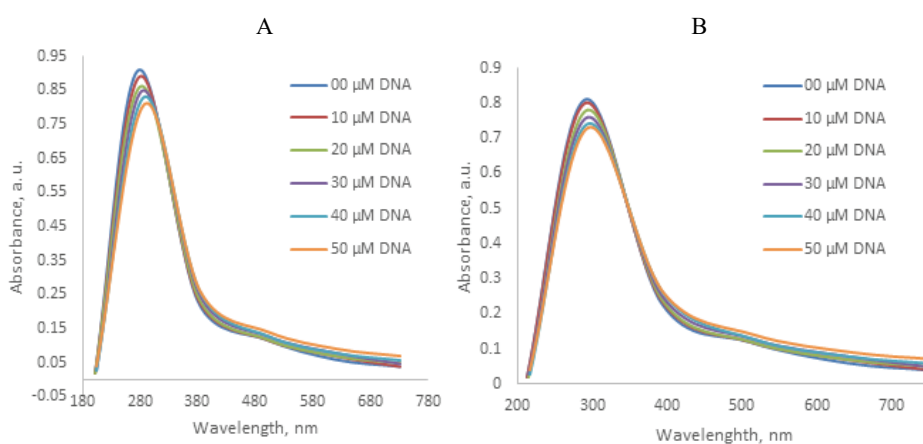


Fig. 5. A) Absorption spectrum of pure complex **1** ($\lambda_{\max} = 277$ nm, absorbance = 0.91) and addition of DNA from 10–50 μ M in downward direction, causing a shift of λ_{\max} to 289 nm and decrease of absorbance (0.91–0.81); B) absorption spectrum of pure complex **2** ($\lambda_{\max} = 289$ nm; absorbance = 0.89) and addition of DNA from 10–50 μ M in downward direction, causing a shift of λ_{\max} to 294 nm and decrease of absorbance from 0.89 to 0.73

Fig. 5B shows the absorption spectrum of complex **2**, showing an absorption band at $\lambda_{\max} = 289$ nm due to π - π electronic transition of the aromatic moiety in the complex and a weak absorption peak at 510 nm due to d-d transition in copper(II) ion. This also corresponds to distorted octahedral geometry where the solvent DMSO is attached at the sixth position to copper ion in the solution form.

DNA binding study through UV/Vis spectrophotometry

UV/Vis spectrophotometer was used for monitoring the variation in λ_{\max} and absorbance of the complexes upon addition of DNA to the solutions of the complexes. The mode of interaction of the complexes with DNA can be judged from the shifts in λ_{\max} . A shift toward shorter wavelength (blue) is an indication of electrostatic interaction, while red shift (shift toward longer wavelength) is the consequences of intercalation.³² However, a very small blue shifts up to 5 nm

and concomitant decrease in absorbance (hypochromism) is an indication of groove binding. The complex **1** showed a small red shift as well as hypochromism as evident from Fig. 5A, that correspond to weaker intercalation mode of interaction of the complex with DNA helix. Similarly, the complex **2** showed a small red shift as well as hypochromism that according to the above discussion is a result of weaker intercalation mode of interaction with DNA as shown in Fig. 5B.

UV/Vis spectroscopy is commonly employed technique for DNA study and their interaction with drugs. The copper(II) complexes do not exhibit any intense d-d or charge transfer band to monitor their interaction with DNA, so the intense ligand base (π - π) absorption band is used to monitor the interaction of complexes with DNA.^{33,34} Both the complexes show a decrease in the intensity (hypochromism) as well as a small red shift (bathochromism), that according to the literature reflect intercalative mode of interaction, which result from the interaction between aromatic ligand and the DNA base pair through stacking interaction. The complex **1** gave peak at 277 nm with absorbance 0.91 in the UV-region due to aromatic moiety; similarly the complex **2** gave peak in UV-region due to phenanthroline at 289 nm with 0.81 absorbance.³⁵

The broad peak in the 500 nm range is due to d-d transition of Cu^{2+} as observed in other copper(II) complexes.³² There is decrease in the absorbance of the peak in UV-region on addition of DNA due to the formation of complex-DNA adduct and a consequent decrease in the concentration of the free complexes. Both the complexes show hypochromic effect as well as red shift, the extent of hypochromic effect and red shift is a measure of the degree of intercalation.³⁶

The extent of interaction of the complexes with DNA was determined quantitatively from the binding constant K_b values through the Benesi-Hildebrand equation³⁷ as expressed below:

$$A_0/(A-A_0) = \varepsilon_G/(\varepsilon_{H-G}-\varepsilon_G) + \varepsilon_G/(\varepsilon_{H-G}-\varepsilon_G)(1/K_b C_{\text{DNA}})$$

The binding constant K_b values of the complexes were calculated from the intercept to slope ratio of the plots of $A_0/A-A_0$ vs. $1/C_{\text{DNA}}$ shown in Fig. 6A and B. K_b values were found out to be 2.0×10^3 and $1.1 \times 10^3 \text{ M}^{-1}$ for complexes **1** and **2**. These values are of comparable magnitude to those of other binuclear copper(II) complexes.⁹ This study indicated that the synthesized complexes bind efficiently with DNA.

The structural stability of synthesized complexes in solution was determined by preparing their 3 mM solution in aqueous DMSO (1:4) and scanning the solution in 400–1100 nm after 1, 3 and 24 h by UV/Vis spectroscopy for investigating their stability. It was observed from Fig. 7 that no change is observed in their λ_{max} for 24 h, which suggest that distorted octahedral geometry around each

copper ion remain constant. However, a small increase in their absorbance was attributed to variation in temperature for 24 h.

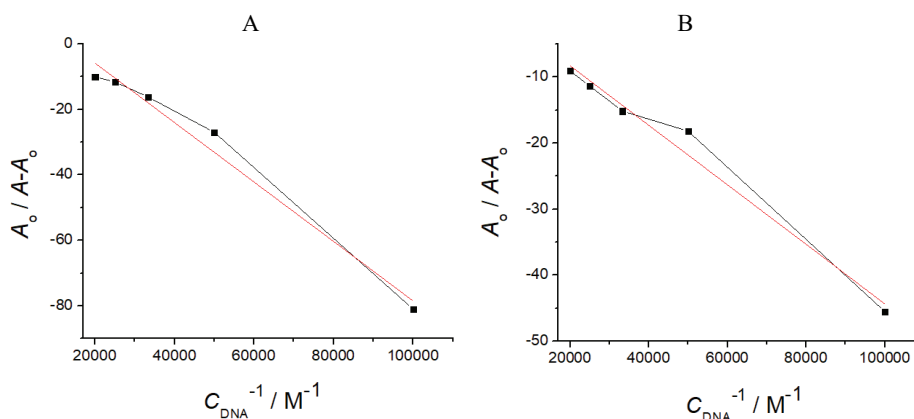


Fig. 6. A plots of $A_0/(A-A_0)$ vs. $1/c_{\text{DNA}}$ for the determination of binding constant of complexes: A) **1**, $K_b = 2.0 \times 10^3 \text{ M}^{-1}$ and B) **2**, $K_b = 1.1 \times 10^3 \text{ M}^{-1}$.

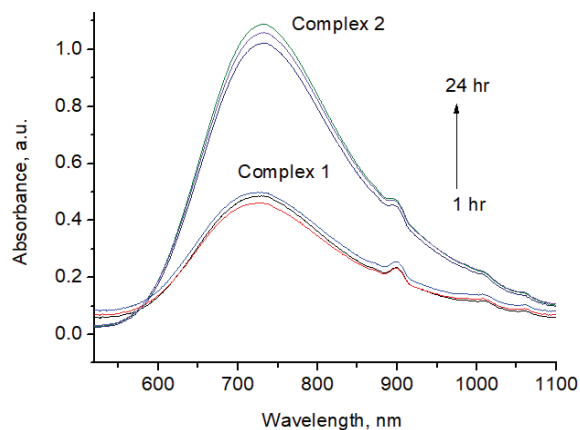


Fig. 7. UV/Vis spectra of complexes **1** and **2** in aqueous DMSO (1:4) in various intervals showing the stable geometry in solution.

Molecular docking studies

To assess the interactions of the synthesized complexes with DNA, docking studies were carried out from which it was observed that the top ranked conformations of both compounds were well interacted with the active residues of the DNA. Among the synthesized compounds, the most active compound is complex **1** on the basis of the docking scores. The docking results showed that the metal-complex derivatives bind to DNA by intercalation, which is the only interaction mode we have obtained by docking. The result of docking of complex **1** with DNA is shown in Fig. 8. As it can be seen the complex **1** showed intercalation with DNA by forming five H-bonds with chain A, being the active resi-

due of the DNA. The docking score of the DNA–complex adduct was -11.6946 . The carbon atom of the ligand form $H-\pi$ interaction with adenine (DA5) and guanine (DG16) residues of the DNA made $\pi-H$ contact with 6-ring moiety of the inhibitor. Metal complexes that bind with DNA primarily by intercalation, are considered the most effective class of molecules as an anticancer drug.^{38–40}

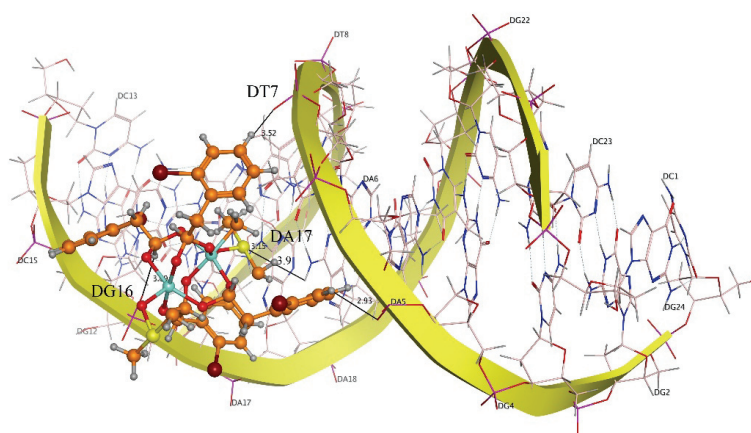


Fig. 8. Docking orientation of complex 1 inside the active site of DNA.

From the docking conformation of the complex 2 (docking score = -10.4301), it was observed that this compound established three polar interactions with active site residues DT7, DG14 and DC15 of DNA, respectively (Fig. 9).

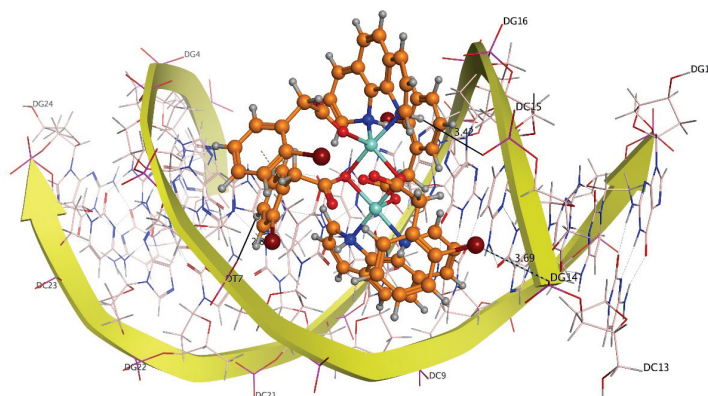


Fig. 9. Docking orientation of complex 2 inside the active site of DNA.

An excellent arrangement was obtained as the best docked pose showed important binding features mostly based on interactions due to various interacting moieties of derivatives, and phosphorus atom including its versatile structural features.

Both the copper complexes bind mainly through groove binding and partly through intercalation by hydrogen bonding with adenine, guanine and π -H contact with 6-ring moiety of the complexes as evident from a small red shift and a small hypochromism.

CONCLUSION

Two new binuclear copper(II) complexes have been synthesized from 2-bromophenyl acetate and 1,10-phenanthroline and characterized by UV/Vis, FT-IR, TGA and X-ray studies. Both complexes have dinuclear structures, in which each Cu(II) is penta-coordinated and has square pyramidal geometry. Complex **1** is paddlewheel while complex **2** is oxygen bridged type. In both complexes the apical and equatorial Cu–O bond lengths are considerably different. The UV/Vis spectroscopy gave K_b values 2.0×10^3 and $1.1 \times 10^3 \text{ M}^{-1}$, respectively for complexes **1** and **2**. The binding activity of both complexes with DNA was determined computationally by molecular docking through MOE software, in which the complex **1** intercalate with DNA by forming five H-bonds with chain A, as well as through H- π interaction with adenine (DA5) and guanine (DG16) residues of the DNA. The complex **2** established three polar interactions with active site residues DT7, DG14 and DC15 of DNA. Both results are in agreement with each other which point out the biological relevance of the synthesized complexes.

SUPPLEMENTARY MATERIAL

Additional data are available electronically at the pages of journal website: <http://www.shd.org.rs/JSCS/>, or from the corresponding author on request.

ИЗВОД

ДИНУКЛЕАРНИ КОМПЛЕКСИ БАКРА(II): СИНТЕЗА, СТРУКТУРНА КАРАКТЕРИЗАЦИЈА, ДНК ИНТЕРАКЦИЈЕ И *in silico* ИСПИТИВАЊА

ABDUL WAHEED KAMRAN¹, SAQIB ALI², MUHAMMAD NAWAZ TAHIR³, MUHAMMAD ZAHOOR¹, ABDUL WADOOD⁴ и MUHAMMAD IQBAL⁵

¹Department of Chemistry, University of Malakand, Chakdara, Dir(L) KPK, Pakistan, ²Department of Chemistry Quaid-i-Azam University Islamabad 45320, Pakistan, ³Department of Physics, University of Sargodha, Sargodha, Pakistan, ⁴Department of Biochemistry, Abdul Wali Khan University Mardan, KPK, Pakistan и ⁵Department of Chemistry Bacha Khan University Charsadda 24420, KPK, Pakistan

Описана је синтеза два нова динуклеарна комплекса бакра опште формуле $[\{\text{Cu}(\text{dmsO})(\mu\text{-L})\}_2\text{Cu}(\text{dmsO})]$ (**1**) и $[\{\text{Cu}(\text{phen})(\text{L})(\mu\text{-L})\}_2\text{Cu}(\text{L})(\text{phen})]$ (**2**) (dmsO је диметил-сулфоксид, L је 2-бромофенил-ацетат и phen је 1,10-фенантролин). Комплекси су окарактерисани помоћу UV/Vis и FT-IR спектроскопије, термогравиметријске/диференцијалне термалне анализе и дифракцијом X-зрака са кристала. Нађено је да се структура комплекса **1** састоји од међусобно повезаних *paddlewheel* комплексних јединица преко 1,2-*O,O*-атома док су у комплексу **2** комплексне јединице повезане преко 1,1-*O*-атома. Израчунате вредности константи везивања за ДНК су 2.0×10^3 (**1**) и $1.1 \times 10^3 \text{ M}^{-1}$ (**2**). Начин интеракције комплекса **1** и **2** са ДНК хеликсом испитиван је методом молекуларског моделирања (*in silico*) МОЕ софтвером. Синтетисани комплекси су структурно и биолошки веома занимљиви.

(Примљено 15. јула, ревидирано 30. септембра, прихваћено 10. октобра 2019)

REFERENCES

1. F. Tisato, C. Marzano, M. Porchia, M. Pellei, C. Santini, *Med. Res. Rev.* **30** (2010) 708 (<http://dx.doi.org/10.1002/med.20174>)
2. T. Aratani, *Pure. Appl. Chem.* **57** (1985) 1839 (<http://dx.doi.org/10.1351/pac198557121839>)
3. P. C. Ford, E. Cariata, J. Bourassa, *Chem. Rev.* **99** (1999) 3625 (<http://dx.doi.org/10.1021/cr960109i>)
4. T. Ohishi, M. Nishiura, Z. Hou, *Angew. Chem. Int. Ed.* **47** (2008) 5792 (<http://dx.doi.org/10.1002/anie.200801857>)
5. G. E. Jackson, L. M. Gama, A. Voye, M. Kelly, *J. Inorg. Biochem.* **79** (2000) 147 ([http://dx.doi.org/10.1016/s0162-0134\(99\)00171-3](http://dx.doi.org/10.1016/s0162-0134(99)00171-3))
6. V. L. Goodman, G. J. Brewer, S. D. Merajver, *Endo. Rel. Cancer* **11** (2004) 255 (<https://doi.org/10.1677/erc.0.0110255>)
7. A. Soroceanu, L. Vacareanu, N. Vornicu, M. Cazacu, V. Rudic, T. Croitori, *Inorg. Chim. Acta* **442** (2016) 119 (<https://doi.org/10.1016/j.ica.2015.12.006>)
8. A. Grodzicki, I. Łakomska, P. Piszczek, I. Szymańska, E. Szlyk, *Coord. Chem. Rev.* **249** (2005) 2232 (<http://dx.doi.org/10.1016/j.ccr.2005.05.026>)
9. M. Iqbal, M. Sirajuddin, S. Ali, M. Sohail, M. N. Tahir, *Inorg. Chim. Acta* **440** (2016) 129 (<http://dx.doi.org/10.1016/j.ica.2015.10.042>)
10. S. Majumder, M. Fleck, C. R. Lucas, S. Mohanta, *J. Mol. Struct.* **1020** (2012) 127 (<http://dx.doi.org/10.1016/j.molstruc.2012.04.003>)
11. T. Hirohama, Y. Kuranuki, E. Ebina, T. Sugizaki, H. Arii, M. Chikira, P. T. Selvi, M. Palaniandavar, *J. Inorg. Biochem.* **99** (2005) 1205 (<http://dx.doi.org/10.1039/b000000x>)
12. K. E. Erkkilä, D. T. Odom, J. K. Barton, *Chem. Rev.* **99** (1999) 2777 (<https://doi.org/10.1021/cr9804341>)
13. N. Shahabadi, M. Falsafi, *Spectrochim. Acta, A* **125** (2014) 154 (<http://dx.doi.org/10.1016/j.saa.2014.01.066>)
14. F. Wightman, D. L. Lighty, *Physiol. Plant.* **55** (1982) 17 (<https://doi.org/10.1111/j.1399-3054.1982.tb00278.x>)
15. B. Cryer, MD, M. Feldman, *Am. J. Med.* **104** (1998) 413 ([https://doi.org/10.1016/s0002-9343\(98\)00091-6](https://doi.org/10.1016/s0002-9343(98)00091-6))
16. Anbu, M. Kandaswamy, *Polyhedron* **30** (2011) 123 (<https://doi.org/10.1016/j.poly.2010.09.041>)
17. S. Anbu, M. Kandaswamy, M. Selvaraj, *Polyhedron* **33** (2012) 1 (<https://doi.org/10.1016/j.poly.2011.10.041>)
18. G. Pratviel, J. Bernadou, B. Meunier, *Adv. Inorg. Chem.* **45** (1998) 251 ([https://doi.org/10.1016/s0898-8838\(08\)60027-6](https://doi.org/10.1016/s0898-8838(08)60027-6))
19. D. Denoyer, S. Masaldan, S. L. Fontaineab, M. A. Cater, *Metallomics* **7** (2015) 1459 (<https://doi.org/10.1039/c5mt00149h>)
20. G. M. Sheldrick, *SHELX Release 97*, 2nd ed., University of Getttingen, Getttingen, 1997
21. L. J. Farrugia, *J. Appl. Crystallogr.* **32** (1999) 837 (<https://doi.org/10.1107/S0021889899006020>)
22. L. J. Farrugia, *J. Appl. Crystallogr.* **30** (1997) 565 (<https://doi.org/10.1107/S0021889897003117>)
23. *Molecular operating environment*, Chemical Computing Group Inc., Montreal, 2016
24. R. Leach, B. K. Shoichet, C. Peishoff, *J. Med. Chem.* **49** (2006) 5851 (<https://doi.org/10.1021/jm060999m>)

25. A. Hangan, A. Bodoki, L. Oprean, G. Alzuet, M. Liu-Gonzalez, J. Borrás, *Polyhedron* **29** (2010) 1305 (<https://doi.org/10.1016/j.poly.2009.12.030>)
26. S. Leconte, R. Ruzziconi, *J. Fluorine Chem.* **117** (2002) 167 ([https://doi.org/10.1016/S0022-1139\(02\)00161-6](https://doi.org/10.1016/S0022-1139(02)00161-6))
27. B. Shen, P. F. Shi, Y. L. Hou, F. F. Wan, D. L. Gao, B. Zhao, *Dalton Trans.* **42** (2013) 3455 (<https://doi.org/10-1039/c2dt32515b>)
28. M. Barquin, M. J. G. Garmendia, S. Pacheco, E. Pinilla, J. M. Seco, M. R. Torres, *Polyhedron* **23** (2004) 1695 (<https://doi.org/10.1016/j.poly.2004.04.013>)
29. M.A. Halcrow, *Chem. Soc. Rev.* **42** (2013) 1784 (<https://doi.org/10.1039/c2cs35253b>)
30. M. Iqbal, S. Ali, A. Haider, N. Khalid, Iran. *J. Sci. Technol. Trans. Sci.* **42** (2018) 1859 (<https://doi.org/10.1007/s40995-016-0141-5>)
31. M. Iqbal, A. Mushtaq, S. Ali, M. Sohail, P. A. Anderson, *Acta Chim. Slov.* **65** (2018) 989 (<https://doi.org/10.17344/acsi.2018.4695>)
32. I. Ucar, B. Karabulut, A. Bulut, O. Buyukgungor, *J. Mol. Struct.* **834** (2007) 336 (<https://doi.org/10.1016/j.molstruc.2006.10.061>)
33. M. Saif, M. M. Mashaly, M. F. Eid, R. Fouad, *Spectrochim. Acta, A* **92** (2012) 347 (<https://doi.org/10.1016/j.saa.2012.02.098>)
34. L. Jia, J. Shi, Z. H. Sun, F. F. Li, Y. Wang, W. N. Wu, Q. Wang, *Inorg. Chim. Acta* **391** (2012) 121 (<https://doi.org/10.1016/j.ica.2012.05.014>)
35. X. Li, Y. T. Li, Z. Y. Wu, Y. J. Zheng, C. W. Yan, *Inorg. Chim. Acta* **385** (2012) 150 (<https://doi.org/10.1016/j.ica.2012.01.047>)
36. T. Hirohama, Y. Kuranuki, E. Ebina, T. Sugizaki, H. Arai, M. Chikira, *J. Inorg. Biochem.* **99** (2005) 1205 (<https://doi.org/10.1016/j.jinorgbio.2005.02.020>)
37. P. T. Selvi, M. Palaniandavar, Y. Ni, D. Lin, S. Kokot, *Anal. Biochem.* **352** (2006) 231 (<https://doi.org/10.1016/j.ab.2006.02.031>)
38. M. Sirajuddin, S. Ali, A. Haider, N. A. Shah, A. Shah, M. R. Khan, *Polyhedron* **40** (2012) 19 (<https://doi.org/10.1016/j.poly.2012.03.048>)
39. A. Draksharapu, A. J. Boersma, M. Leising, A. Meetsma, W. R. Browne, G. Roelfes, *Dalton Trans.* **44** (2015) 3647 (<http://doi.org/10.1039/C4DT02733G>)
40. J. K. Barton, E. D. Olmon, P. A. Sontz, *Coord. Chem. Rev.* **255** (2011) 619 (<https://doi.org/10.1016/j.ccr.2010.09.002>).